Hydrothermal synthesis of high-performance nitrogen-doped carbon quantum dots from *Ophiopogon japonicus* and their application in sensing Fe (III) with a broad quantitative range

Y. J. Sun[a], J. S. Tang[a,b, *], L. Xiang[a], X. Hu[a], J. Wei[c], X. J. Song[d]
[a]Department of environmental and energy engineering, Anhui Jianzhu University.
[b]Anhui Provincial Key Laboratory of Environmental Pollution Control and Resource Reuse, Anhui Jianzhu University
[c]School of Public Health, Anhui Medical University
[d]School of Materials and Chemical Engineering, Anhui Jianzhu University

In this work, the leaves of *Ophiopogon japonicus* and melamine were used as precursors and nitrogen source for preparing nitrogen-doped carbon quantum dots (N-CQDs)，its fluorescence quantum yield of 10.6%, have strong emission wavelength (320nm), and shows good stability. Owing to electron transfer and exchange between Fe^{3+} ions and N-CQDs, the fluorescence of N-CQDs was only quenched by Fe^{3+} ions. The N-CQDs have been used as a fluorescence sensor, which had widely selective concentration range (0 ~ 600 μmol/L) and with a 1.151 μM limit of detection (LOD), for the detection of Fe^{3+} ions. Importantly, this sensor has successfully been applied to the quantitative detection of Fe^{3+} ions in actual water samples.

1. Introduction

Carbon quantum dots (CQDs), which have advantages of inexpensive, stability, good biocompatibility, photobleaching resistance, low toxicity and environmental friendliness, have been widely developed for chemical sensing[1], bioimaging[2], nanomedicine and batteries[3, 4]. As a material with unique optical properties, CQDs have been showed excellent application in measurement of various metal ions, due to good water-solubility and superior chemical-stability. Compared with other methods, the synthesis of CQDs from biological materials or industrial wastes has the advantages of low cost, non-toxic, renewable and so on, which is conducive to large-scale production. In addition, its is environment friendly, does not require the use of toxic solvents and produce toxic by-products[5].

In response to the concept of sustainable development of the United Nations, the frontier technology of material science had utilized biological materials and industrial waste as precursors to green synthesize CQDs, such as allium fistulosum[6], rose-heart radish[7], garlic[8],

---

banana peel[9], biorefinery waste[10], and wood chips etc[11]. Due to some natural materials containing single compounds, the fluorescence intensity of prepared CQDs were affected by surface defects that resulted in low fluorescence quantum yield (QY). Therefore, it is necessary to improve the optical properties by doping a variety of heteroatoms such as metal and non-metal atoms. The doping of metal atoms is restricted, as a result of the inefficiency, uneven doping[12], and environmental pollution[13]. Doped non-metallic heteroatoms can improve the fluorescence quantum yield of CQDs by affecting the band gap and electron density[14]. Nitrogen atoms hae a similar atomic size to the carbon atoms in CQDs and could bond with carbon atoms to form strong covalent bond[15]. Accordingly, nitrogen atoms are commonly used in the doping of carbon nanomaterials.

The fluorescence quantum yield of CQDs, prepared from plant leaves with carbon oxide and protein as main components, was low. *Ophiopogon japonicus* (Liliaceae), a traditional Chinese medicinal plant, the main components of leaves include carbon oxides and proteins, which can be hydrolyzed into monosaccharides and various amino acids[16,17]. In this work, nitrogen-doped carbon quantum dots (N-CQDs) were synthesized by one-pot hydrothermal method by using the leaves of *O. japonicus* and melamine as precursors and nitrogen source (Fig. 1). The prepared N-CQDs have good water solubility, emit bright blue fluorescence under the irradiation of ultraviolet lamp, and have strong selectivity for Fe^{3+} ions, can be used as a fluorescent probe for the quantitative detection of Fe^{3+} ions in water. In addition, the photoluminescence mechanism and quenching mechanism of N-CQDs were investigated and discussed.
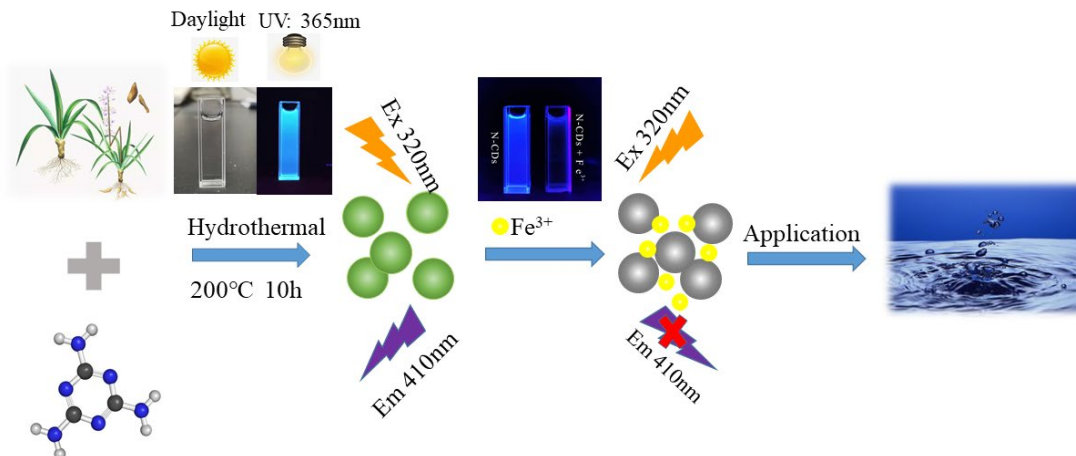

Fig. 1. N-CDs were synthesized by hydrothermal method for the determination of Fe^{3+} in water samples.

2. Experimental

2.1. Materials

The leaves of *O. japonicus* were obtained from the campus of Anhui Jianzhu University. Quinine sulfate (Sigma-Aldrich, 99%), eight different nitrogen-containing substances (Lysine, Melamine, 2-2bipyridine, Diphenylazocarbazide, Aminosulfonic acid, Chitosan, Antipyrine, Dopamine hydrochloride) and eighteen metal salts ($CaCl_2$, $NiCl_2$, $CoCl_2$, $CdCl_2$, $FeSO_4 \cdot 7H_2O$, $FeCl_3$, $AgNO_3$, $ZnCl_2 \cdot 6H_2O$, $MnCl_2$, $CuCl_2 \cdot 2H_2O$, $HgSO_4$, $MnCl_2 \cdot 2H_2O$, $ZnSO_4 \cdot 7H_2O$, $Pb(NO_3)_2$, $MgSO_4 \cdot 7H_2O$, NaCl, $Bi(NO_3)_3 \cdot 5H_2O$, LaN_3O_9 and KCl) were purchased from Sinopham. Configuration of Britton-Robison buffer and deionized water prepared in laboratory.

2.2. Preparation of N-CDs

Thoroughly washed the soil and dust on the *O. japonicus* leaves surface with pure water. Then, we put it into the oven until dry and used a high-speed crusher grind dried *O. japonicus* into powder. 0.5g leaf powder of *O. japonicus*, melamine in different proportions (specific description in subsequent section) and 30mL deionized water were placed in a Tefon-lined autoclave and heated at 180℃ for 10 hours. After cooling, the solution wascentrifuged at 10000r/min for 20 minutes, and the impurities were filtered out with a 0.22μm membrane. Finally, the purified N-CQDs solution was put into a sealed volumetric flask in a dry and cool place.

2.3. Apparatus and characterization

The morphology of N-CQDs was analyzed by transmission electron microscope (TEM; JEOL JEM-2100F). The UV absorption spectrum (Uv-3600 UV-vis-NIR spectrophotometer, Shimadzu), fluorescence spectrum (Hitachi F-7000 fluorescence spectrometer) were used to analyze the optical properties of N-CQDs. The elemental composition of N-CQDs was analyzed by X-ray photoelectron spectroscopy (XPS; semeron escalab 250xi), X-ray diffraction (XRD, D/max) and Fourier transform infrared spectrum (FTIR 2500 spectrometer). Its luminescent properties under ultraviolet light were observed by three-way ultraviolet analyzer (zf-20d). The fluorescence lifetime was measured by Edinburgh instrument FLS980.

2.4. Fluorescence analysis of metal ions

Here, we tested the selectivity of N-CQDs to metal ions. The preconfigured concentration is 1000 μmol/L standard solution of 18 metal ions. Take 19 10mL centrifuge tubes (one of which is blank) and add 1mL standard solution of metal ions, respectively. In order to reduce the pH fluctuation caused by metal ion hydrolysis, added 880μL of BR solution, and finally added 20μL of N-CQDs solution so that the metal ion concentration in the mixed solution is 100μmol/L. After reacting at room temperature for 20 minutes, the fluorescence spectrum was tested to observe the response of different ions to N-CQDs, and the specific metal ions were selected.

2.5. Calculation of quantum yield

The QY of N-CQDs was tested according to previous reports[18]. The QY is calculated according to equation (1)[19]. The Quinine sulfate (QY = 0.54) was dissolved in 0.1M H_2SO_4 solution as the standard sample.

$$\Phi_{N-CQDs} = \Phi_{QS} \times \frac{I_{N-CDs}}{I_{QS}} \times \frac{A_{QS}}{A_{N-CQDs}} \times \frac{\eta^2_{N-CQDs}}{\eta^2_{QS}} \tag{1}$$

Φ_{QS} and Φ_{N-CQDs} represent the QY of quinine sulfate and N-CQDs, respectively, and I_{QS} and I_{N-CQDs} represent the measured integral fluorescence intensity of quinine sulfate and N-CQDs, respectively, η_{QS} and η_{N-CQDs} represents the refractive index of quinine sulfate and N-CQDs, and A_{QS} and A_{N-CQDs} represent the optical density of quinine sulfate and N-CQDs.

2.6 Actual water sample detection

For the further applications of N-CQDs sensor for Fe^{3+} determination, we used standard addition method to test three actual water samples. Tap water, mineral water and river water were taken from the faucet of the laboratory, the supermarket of the school and Lake Yi on the southern campus of Anhui Jianzhu University, respectively. All water samples were centrifuged at 15000 rpm for 10 minutes and then filtered through a 0.22μM membrane to remove the suspended particles. The fluorescence spectra of all solutions were tested under 320nm excitation. In order to reduce the instrument and operation error, all solutions were tested three times, and the average value of their fluorescence intensity was calculated as the final test result.

3. Results and discussion

3.1. Synthesis and characterization
3.1.1. Optimization of synthesis conditions

To obtain the best luminescent performance of N-CQDs, the reaction time, this study optimized the mass ratio of raw materials and reaction temperature. The fluorescence intensity of N-CQDs clearly increases when reaction time increases from 2 to 10 hours (Fig. 2a). The longer the reaction time, the more complete doped carbon source and nitrogen source. When the reaction time was more than 10 hours, the fluorescence intensity of N-CQDs decreased slightly. its may be that carbon source and nitrogen source have completely reacted and the reaction provides high temperature continues. All the above factors lead to excessive carbonization and the fluorescence intensity of N-CQDs decreases. Meanwhile, the fluorescence intensity of N-CQDs increases with the amount of nitrogen source. When the quality of nitrogen source exceeds the leaves powder of *Ophiopogon japonicus*, the fluorescence intensity of N-CQDs begins to decrease and its may be caused by different surface groups of carbon source (Fig. 2b).
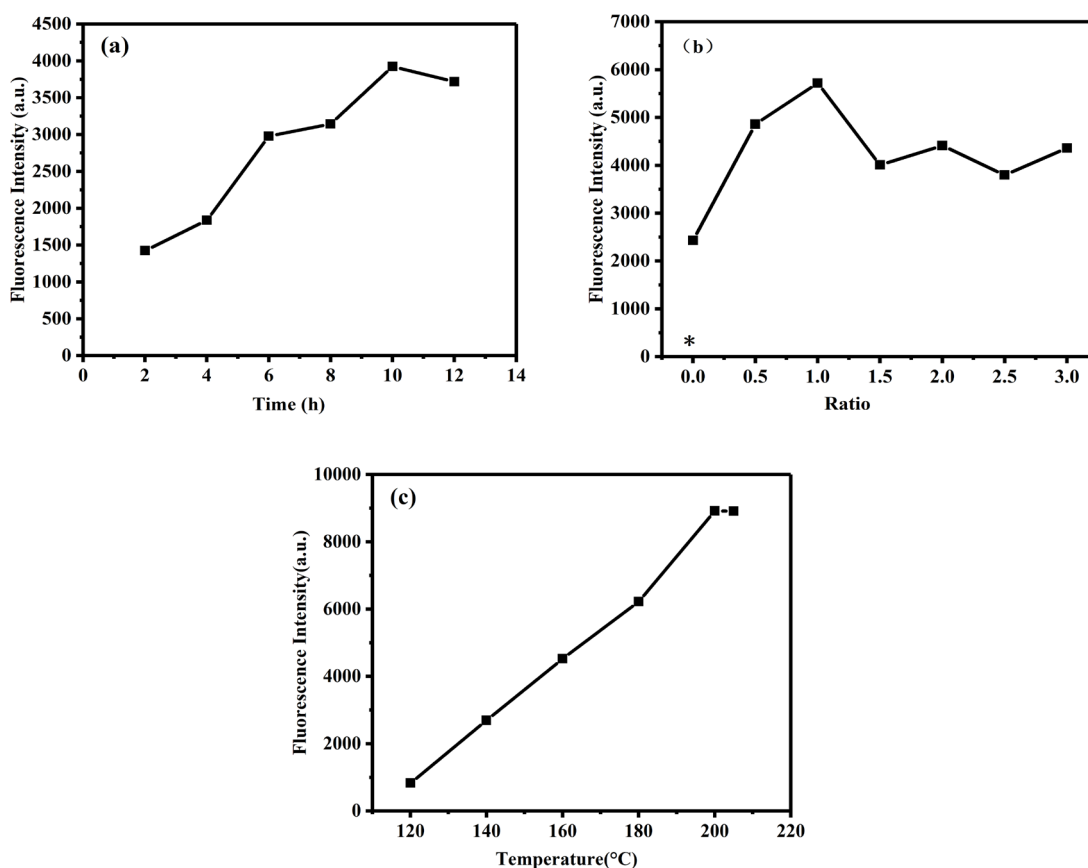

Fig. 2. (a) Optimization of reaction time (the reaction time at 2 hours, 4 hours, 6 hours, 8 hours, 10 hours and 12 hours respectively). (b) Optimization of raw material mass ratio (Take Ophiopogon japonicus powder 0.5g, the mass ratios of Ophiopogon japonicus powder to melamine were 0, 0.5, 1, 1.5, 2, 2.5 and 3, respectively; * represents only have melamine). (c) Optimization of reaction temperature (the reaction temperature at 120°C, 140°C, 160°C, 200°C, 205°C).

Finally, the reaction temperature was optimized. The fluorescence intensity of N-CQDs increases continuously with the increase of temperature and the fluorescence intensity decreases when it reaches 200°C (Fig. 2c). Therefore, the optimal reaction conditions were determined: the reaction time is 10 hours, the reaction ratio is 1 and the reaction temperature is 200°C.

3.1.2. Morphology and optical properties

The size and morphology of N-CQDs were estimated by TEM (Fig. 3a), the approximately spherical N-CQD particles with a particle size of 1-4.5nm have good dispersion in water and the average particle size is 3.4nm (Inset of Fig. 3a). An XRD pattern of N-CQDs (Fig. 3c) showed three sharp diffraction peaks ($2\theta=22.04°$, $26.39°$ and $30.06°$) and three small diffraction peaks ($2\theta=16.87°$, $34.25°$ and $41.99°$), which indicates that the carbon of N-CQDs is composed in a considerably random fashion. Due to the large number of oxygen-containing groups in N-CQDs, the crystallinity of N-CQDs is poor[20]. The FTIR spectrum (Fig. 3d) of the CQDs and N-CQDs confirm its surface functional groups. The wide peak (3421nm) was the stretching vibration of -OH and -NH, that its indicated the existence of hydroxyl and amino groups both in N-CQDs and CQDs[21, 22, 23, 24, 25]. The N-CQDs and CQDs peaks (2927, 1626 and 1030 cm^{-1}) are attributed to C–H, C=O and C–O–C stretches[26]. The weak peaks (1401 cm^{-1}) is attributed to C–N on the surface of N-CQDs[27], which shows that the addition of melamine promotes the formation of C-N bond. The XPS spectra of CQDs and N-CQDs determines the changes of chemical composition before and after its dops nitrogen source. The survey scans of CQDs and N-CQDs(Fig. 4a) showed that CQDs had C (53.46%), O (18.94%), and N (16.82%) and N-CQDs had C (58.90%), O (15.34%), and N (23.58%). All show that the addition of melamine increases the nitrogen content of N-CQDs and improves the fluorescence intensity. The fitting results of C1s, N1s and O1s spectra of CQDs and N-CQDs (Fig. 4b-4g) are shown in Table 2[28, 29].
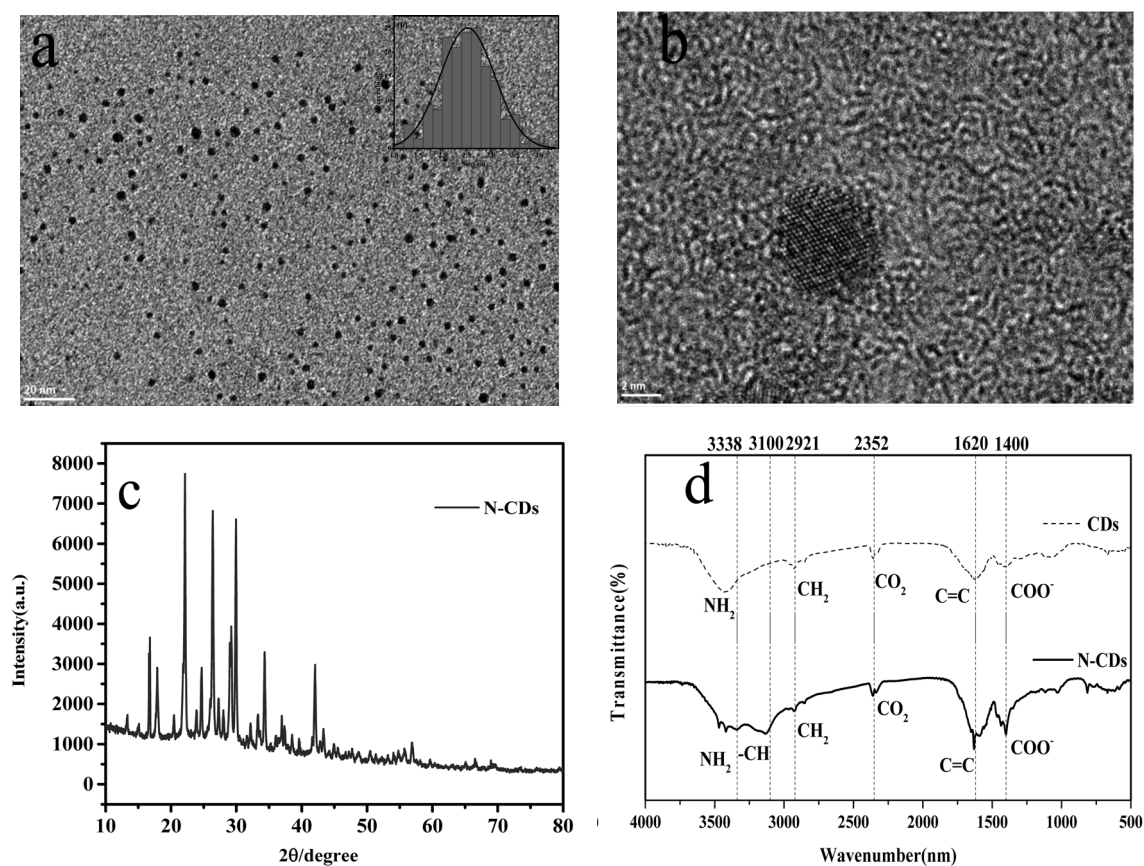

Fig. 3. (a) TEM of N-CDs, (b) The particle size distribution histogram, (c) XRD pattern of N-CDs, and (d) FTIR spectra of N-CDs.

By contrast, the addition of melamine may lead to the conversion of C=C bond of N-CQDs into C-C bond and C=N bond to C-N bond, which results in the increase of carbon content and nitrogen content, changes the valence bond of nitrogen atom and improves the fluores-

cence intensity of CQDs. Based on the XRD, FTIR and XPS spectra, the functional groups on the surface of N-CQDs are C-OH, -NH, C=O, C-O-C and C-N.

Table 1. The fitting results of C1s spectra, N1s spectra and O1s spectra of CDs and N-CDs.

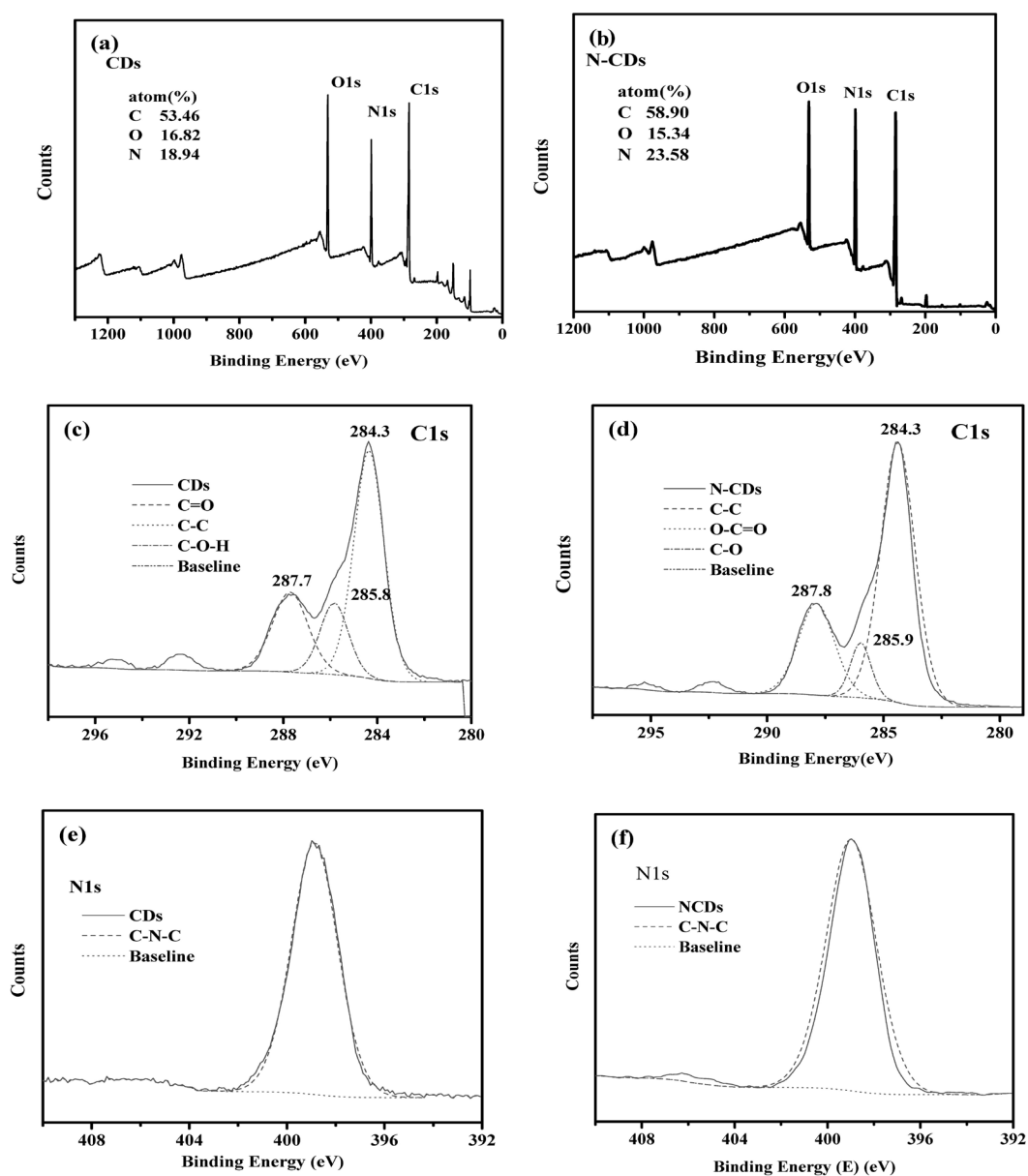|		CDs	N-CDs	Refs
C1s		C-C/C=C(284.3eV)	C-C (284.3eV)	[7]
		-O=C-O (287.8eV)	C=O (287.7eV)	[20]
		C=N/C-C(285.9eV)	C-N/C-OH(285.8eV)	[37]
O1s		C=O (531.8eV)	C-OH(531.6eV)	[33]
		C–O-C (530.5eV)	C-O-C (530.4eV)	[39]
N1s		C-N-C (398.9eV)	C-N-C (398.8eV)	[40]

Fig. 4.1. XPS spectra of CDs, (a) Survey of CD, (b) Survey of N-CDs, (c) C1s of CD, (d) C1s of N-CD, (e) N1s of CD, (f) N1s of N-CD
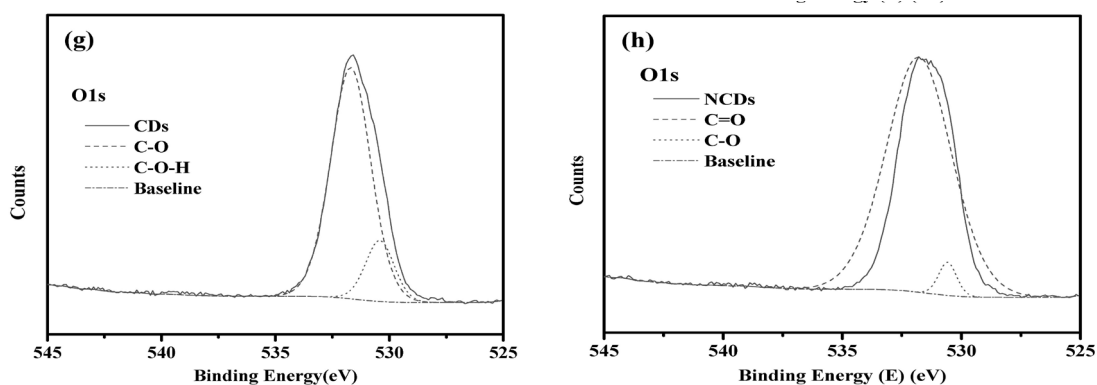
Fig. 4.2. XPS spectra of CDs, (g) O1s of CD, (h) O1s of N-CD.

The optical properties of the prepared N-CQDs were characterized. The emission spectra of N-CQDs at different excitation wavelengths of 220 ~ 400 nm in Fig. 5a. The fluorescence intensity of the emission peak gradually decreases and redshifts when the excitation wavelength increases from 320nm to 400nm. The fluorescence intensity of the emission peak at the excitation wavelength of 320 nm reaches the maximum. The optimum emission and excitation wavelength are 410 nm and 320 nm, a weak absorption peak at 271 nm in Fig. 5b, the electron undergoes n-π* transition, related to the C=O bond contained in the N-CQDs structure[30]. A very bright blue fluorescence in N-CQDs solution under 365 nm ultraviolet light (Fig. 5b). The fluorescence intensity of N-CQDs decreases obviously after adding 100μmol/L Fe^{3+} (Fig. 5c), indicating that the prepared N-CQDs has a good response to Fe^{3+} and used as a fluorescent probe of Fe^{3+}.The fluorescence intensity of N-CQDs is more than double that of undoped CQDs (Fig. 5d). Eight compounds were used as nitrogen sources to prepare N-CQDs (Fig. 6), the N-CQDs synthesized by melamine and leaves of *Ophiopogon japonicus* had the highest fluorescence intensity with a fluorescence quantum yield of 10.6%. Table 3 summarizes the QY of N-CQDs prepared from other green sources[31-39].
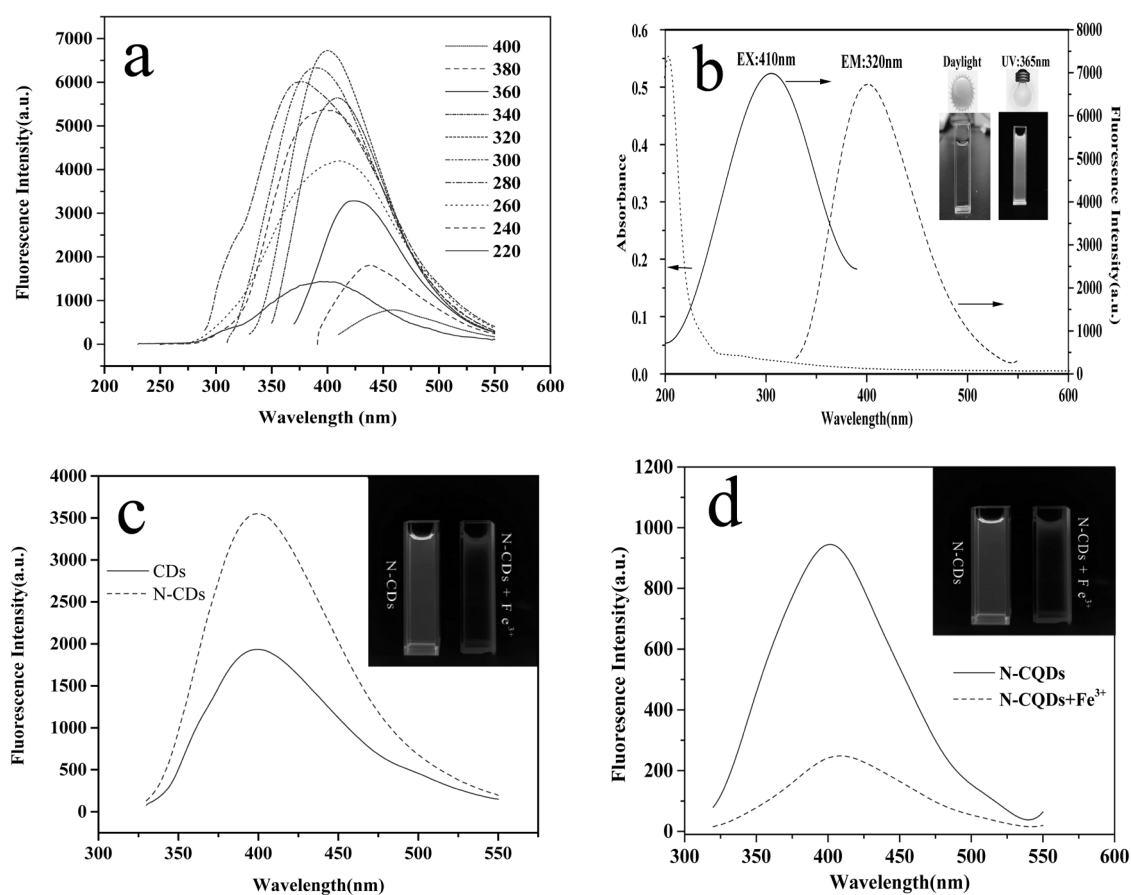
Fig. 5. (a) Emission spectra of the N-CDs at different excitation wavelengths (220~400nm). (b) Absorbance, excitation and emission spectra of the N-CDs. (The insets photos are N-CDs under daylight and UV light). (c) Emission spectra for N-CDs and CDs. (The inset photos are the N-CDs and CDs solutions illuminated under UV light of 365nm). (d) Emission spectra of N-CDs with and without 100mg/L Fe^{3+}. (The inset photos are N-CDs with and without 100mg/L Fe^{3+} solutions illuminated under UV light of 365nm).
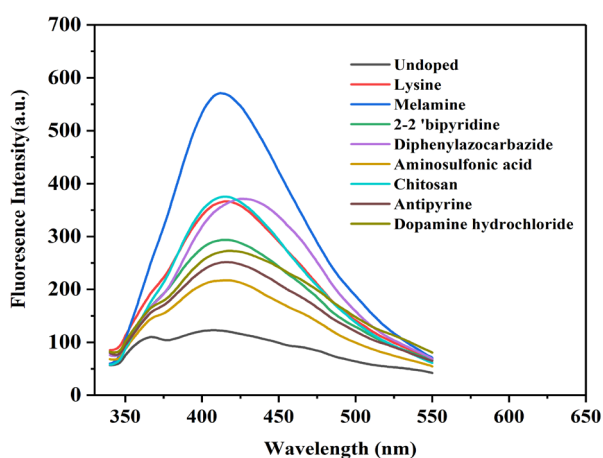

Fig. 6. Eight different nitrogen-containing substances.

Table 2. Fe^{3+} detection of N-CDs compared with other reported CDs and N-CDs.

Sensors	Carbon Precursor	QY(%)	Performances		R^2	Reference
			LOD (μM)	Linear range (μM)		
CDs	Betel leafs	--	--	0.05~0.15	0.9944	[21]
CDs	Mexican Mint	17	0.53	0~15	0.9111	[22]
N-CDs	watermelon juice	10.6	0.16	0~300	0.9811	[23]
CDs	lychee waste	23.5	0.0236	0.1~1.6	0.9998	[24]
CDs	Kumquat	0.08	0.70	0~40	0.9938	[25]
CDs	Fish scale	6.9	0.54	1~78	0.998	[26]
N-CDs	Matrimony vine	30.7	2.22	5~60	0.73003	[27]
CDs	sweet potato	8.64	0.32	1~100	0.9967	[28]
CDs	seville orange	13.3	0.53	33~133	0.99	[29]
N-CDs	*Ophiopogon japonicus* leaves	10.6	1.15	10~600	0.9817	Present work

3.1.3. Stability of N-CQDs

The effects of pH, temperature and ionic strength on the stability of N-CQDs were discussed. The fluorescence intensity of N-CQDs has no significant effect in the range of NaCl concentration from 0 to 1mol/L (Fig. 7a), indicating that N-CQDs can detect Fe^{3+} in physiological environment. The fluorescence intensity of N-CQDs solution can basically remain unchanged when the pH value is in the range of 2.0 ~ 8.0 (Fig. 7b).The fluorescence intensity of N-CQDs solution tends to be stable in the temperature range of 0 ~ 40 °C (Fig. 7c). The above fully shows that the prepared N-CQDs has sufficient stability.
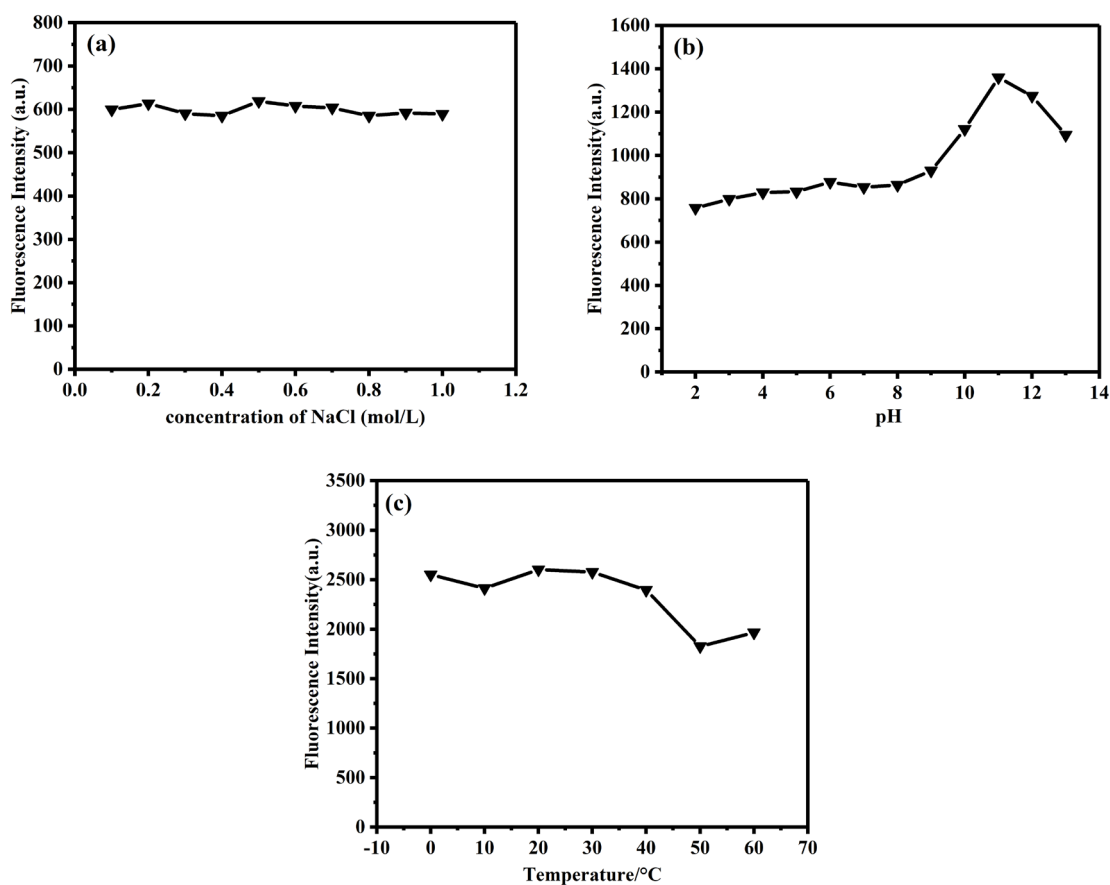
Fig. 7. (a) The fluorescence intensity of N-CDs under different concentrations of NaCl (0.1 ~ 1.0mol/L). (b) The fluorescence intensity of N-CDs under different pH values. (c) The fluorescence intensity of N-CDs under different temperature (0 ~ 60°C).

3.2. Selective detection of metal cations

In order to study the selectivity of N-CQDs as a fluorescent probe, 18 different metal ions were added to N-CQDs solution, to record the fluorescence intensity of N-CQDs under the action of metal ions at the emission wavelength of 320nm. The fluorescence intensity of N-CQDs decreased by about 80% (compared with the original solution) (Fig. 8a) when Fe^{3+} was added into N-CQDs solution, indicating the N-CQDs has strong selectivity for Fe^{3+} ions.
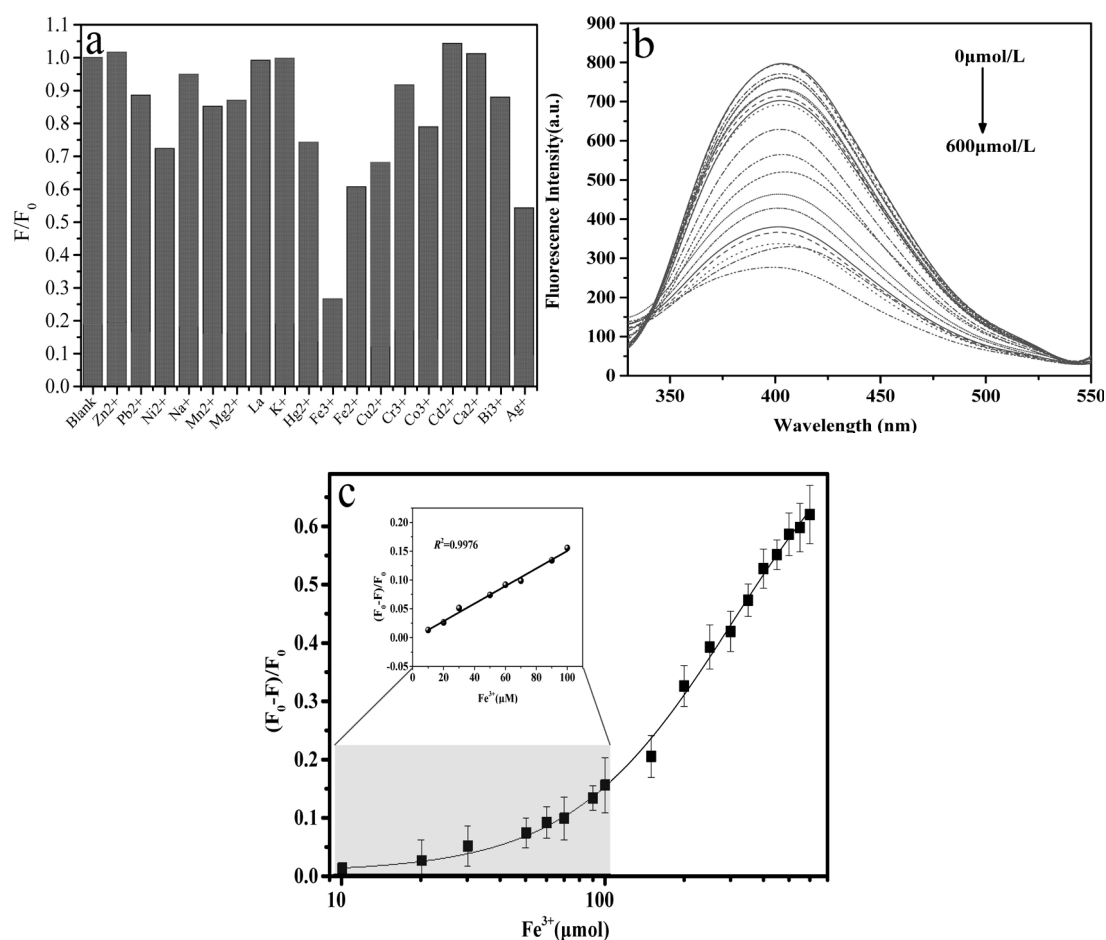
Fig. 8. (a) Fluorescence intensity of N-CDs with different metal ions at 100μmol/L. F and F_0 are the fluorescence intensity of N-CDs with and without different metal ions, respectively. (b) Emission spectra of N-CDs upon addition of Fe^{3+} with different concentrations. (c) The plot of the fluorescence quenching factor ((F_0–F)/ F_0) versus concentrations of Fe^{3+} and relevant linear regions.

3.3. Optimizing the detection conditions of N-CQDs for Fe^{3+}

For achieving the best sensing performance of the N-CQDs based fluorescent probes for Fe^{3+} ions, some crucial experimental parameters including incubation time, solution pH were optimized. After adding 50μmol/L Fe^{3+} ions solutions, the fluorescence intensity of N-CQDs totally quenched quickly and stabilized after 30s (Fig. 9a). The fluorescence intensity of the mixed solution of N-CQDs and Fe^{3+} remains basically stable when the pH changes from 2.0 to 9.0, increases and then decreases when the pH changes from 9.0 to 13.0, reaches the maximum when the pH is 11 (Fig. 9b). Considering that Fe^{3+} ions is easy to form insoluble and unstable iron hydroxide under alkaline conditions,[40] the pH selected for subsequent experiments is 3.0. The above observation results show that the fluorescence intensity of N-CQDs totally quenched by Fe^{3+} ions under the pH of 3.0 for 30s.
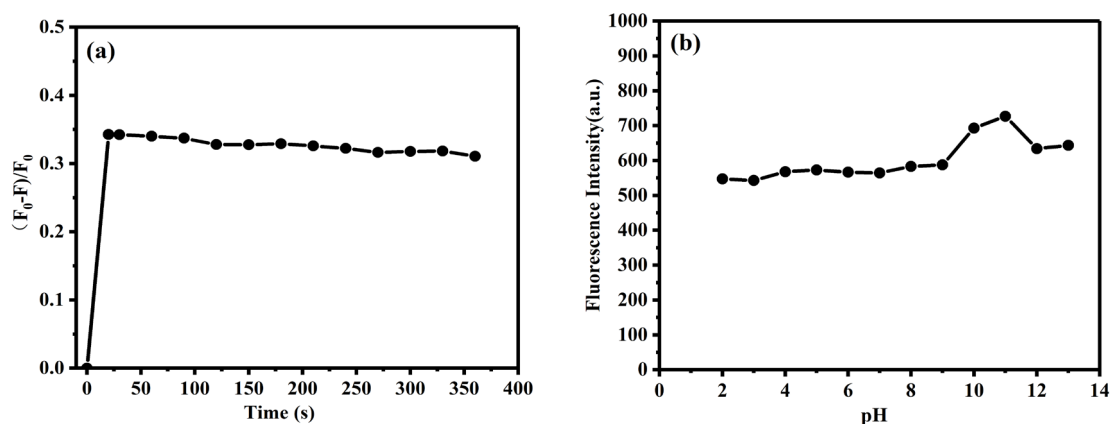
Fig. 9. (a) Incubation time versus fluorescence intensity of N-CDs, the F_0 and F were the fluorescence intensities with and without 50µmol/L Fe^{3+}, respectively. (b) Effect of pH on fluorescence intensity of N-CDs and Fe^{3+} mixed solution.

3.4. Sensitivity assay of N-CQDs

The system clearly reflected the quenching effect of the addition of Fe^{3+} on the fluorescence. Fluorescence quenching factor versus the concentrations of Fe^{3+} was used to calculate regression equation according to equation (2) of

$$\frac{F_0-F}{F_0} = aC_{Fe^{3+}} + b \qquad (2)$$

where F_0 and F are the fluoresence intensities in the absence and presence of Fe^{3+}, respectively. $C_{Fe^{3+}}$ is the concentration of Fe^{3+}. a and b are the equation coefficients.

The linear relationship between the concentration of $(F_0–F)/F_0$ and $C_{Fe^{3+}}$ was $(F_0–F)/F_0$ =$0.00869+0.00122C_{Fe^{3+}}$ (µmol/L). And the range of detection Fe^{3+} was from 10 to 100µmol/L with a correlation coefficient (0.9976) (Fig. 6b and c insert Figure). The limit of detection (LOD) was calculated using equation of $LOD = \frac{3\sigma}{S}$[41], where σ is the value of standard deviation and s is the slope of the linear fit. The calculated LOD was 1.151 µM for the prepared N-CQDs.

The logistic equation of 4S parameters is often used to fitting strategies in quantitative analyze. This quantitative mean can effectively extend the quantitative threshold of Fe^{3+} detection. The dose-response curves showed in Fig. 6c was calculated as

$$F(x) = \frac{A-D}{1+(\frac{x}{C})^B} + D \qquad (3)$$

where F(x) is the response value $((F_0–F)/F_0)$, A is the max response value in the present of target at the highest concentration, D is the least response value without target, B is slope, and C is target concentration corresponding half response effect. The correlation coefficient of 0.9985 was obtained using the 4S parameters logistic formulation to fitting the relationship between logarithm of Fe^{3+} concentration and fluorescence quenching percentage. It is noteworthy that

N-CQDs outperform most previously reported CQDs and N-CQDs for Fe^{3+} detection linear range (Table 3).

3.5 Actual water sample detection

Fe^{3+} ions were seriously quenched the fluorescence of N-CQDs, use N-CQDs to detect the concentration of Fe^{3+} ions in actual samples (three sources of water) to verify the accuracy of this method. The experimental results (Table 4) showed that the relative standard deviation (RSD) of Fe^{3+} ions was less than 4.55% and the recovery rate of Fe^{3+} ions was 97.2% ~ 111%, further proving that the N-CQDs can be used as a fluorescent probe for the detection of Fe^{3+} and has a certain practical application value.

Table 4. Determination of Fe^{3+} in real water samples (n=3).

Samples	Added (μmol/L)	Found (μmol/L)	Recovery (%)	RSD (%)
Tap water	10	11.10	111.00	2.14
	30	31.08	103.60	3.23
	50	51.00	102.00	1.42
Mineral water	10	9.86	98.60	3.15
	30	31.33	104.40	2.44
	50	49.78	99.56	2.76
River water	10	9.72	97.20	4.55
	30	33.33	111.10	3.87
	50	52.11	104.22	3.48

3.6. Mechanism for Fe^{3+} detection by N-CQDs

At present, the main reasons for fluorescence quenching of luminescent substances are as follows[42]: (1) Static quenching: fluorescence quenching is mainly caused by the formation of ground state complexes between luminescent substances and other substances; (2) Dynamic quenching: fluorescence quenching caused by energy transfer due to diffusion and collision between luminescent substances and other substances.

The common method to judge whether the quenching is static quenching or dynamic quenching is to test the fluorescence lifetime before and after the reaction. Therefore, we tested the fluorescence lifetime of N-CQDs with and without Fe^{3+} (Fig. 10b), the fluorescence lifetimes of the two solutions are 8.34ns, 7.59ns, respectively (Table 5). The fluorescence lifetime of the N-CQDs reduced by about 8.9% after the addition of 50μmol/L Fe^{3+}, indicating that fluorescence probing belongs to the dynamic quenching, and the reduced lifetime indicates an ultra-fast N-CQDs/Fe^{3+} electron-transfer process and leads to quenching.

Table 5. Fluorescence lifetime fitting results.

	τ_1(ns)	τ_2(ns)	B_1	B_2	$\tau_{(avers)}$(ns)
N-CDs	2.5178	10.9517	206.209	105.990	8.3452
N-CDs+Fe^{3+}	2.4103	9.7113	227.348	138.606	7.5989

This inference was confirmed in the following UV absorption spectrum test. N-CQDs and Fe^{3+} pure solutions have an absorption peak at 271 nm and 290 nm (Fig. 10a), respectively. The two absorption peaks of 271nm and 290nm can be found in the UV absorption spectrum of the mixture of N-CQDs and Fe^{3+}. But there are no other absorption peaks are produced, which indicates that N-CQDs and Fe^{3+} do not form a complex in the ground state, which also indicates that the type of fluorescence quenching of N-CQDs caused by Fe^{3+} belongs to dynamic quenching. In addition, the ultraviolet absorption spectrum of Fe^{3+} overlaps with the fluorescence spectrum of N-CQDs, which further indicates that the fluorescence quenching of N-CQDs by Fe^{3+} belongs to the process of electron transfer. However, the process of electron exchange and energy transfer accounts for a relatively small proportion in this process. The ion selective chemical structure contained in carbon quantum dots can promote electron/hole recombination through an effective electron transfer process. For example, quinoline and acridine contain a large number of nitrogen-containing functional groups, which can form some pyridine heterocyclic compounds[43]. These fluorescent groups belong to the selective chemical structure of iron ions and play a very important role in the selection of iron ions. These fluorescent groups belong to the selective chemical structure of iron ions and play an important role in the selection of iron ions. The fluorescence quenching of N-CQDs by Fe^{3+} was promoted by the electron transfer between these nitrogen-containing groups and iron ions. In the previous characterization process, N-CQDs may contain structures similar to them. Because of electron transfer and exchange, the fluorescence intensity of N-CQDs was quenched by Fe^{3+} ions and the proportion of its is needed further research. (Fig. 11). Therefore, it is feasible and reliable to construct a fluorescence sensing system based on N-CQDs for sensitive detection of Fe^{3+} ions.
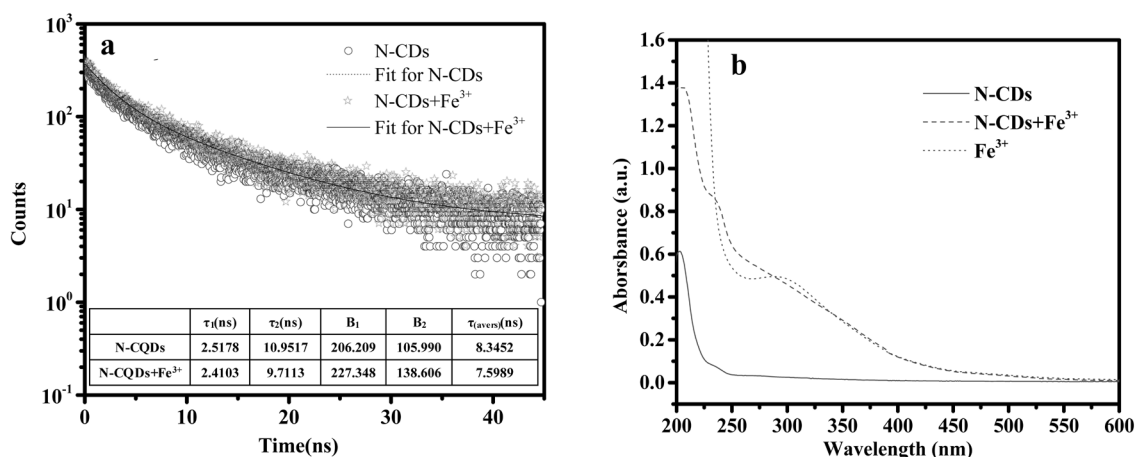

Fig. 10. (a) The fluorescence lifetime curves of N-CDs with and without 50μmol Fe^{3+}. (b) UV absorption spectra of N-CDs, N-CDs/Fe^{3+}, Fe^{3+}.
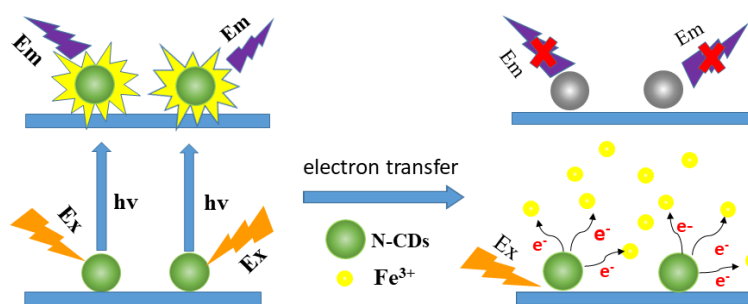
Fig. 11. Sensing mechanism of N-CDs to Fe^{3+}.

4. Conclusions

In general, we had prepared N-CQDs by a green method that is hydrothermal treatment of leaves (*Ophiopogon japonicus*) with melamine modification. The fluorescence QY of N-CQDs with excellent luminescence characteristics and good stability is optimized as high as 10.6%, which is superior to most previous CQDs. In addition, the fluorescence intensity of N-CQDs could be selectively quenched by Fe^{3+} ions. The fluorescence quenching mechanism of N-CQDs by Fe^{3+} ions belongs to the dynamic quenching and it was successfully used as a selective probe for Fe^{3+} detection. Under the optimized conditions, the fluorescence intensity of N-CQDs demonstrated a good linear relationship with the concentration of Fe^{3+} ions in the range of 10 ~ 600μmol/L, and the LOD is 1.151μM. It can be used for the quantitative detection of Fe^{3+} ions in actual water samples. In the application of quantitative detection of Fe^{3+} ions in actual water samples, the relative standard deviation (RSD) of Fe^{3+} ions concentration is less than 4.55% and the recovery is 97.2% ~ 111%. Therefore, this study has realized high efficiency, green, simple, convenient and cheap preparation of N-CQDs.

Acknowledgements

References

[1] Y. L. Shi, W. Shen, Z.Q. Gao. Chem. Soc. Rev. 44, 362(2015);
https://doi.org/10.1039/C4CS00269E
[2] M. J. Youh, M. C. Chung, H. C. Tai, C. Y. Chen, Y. Y. Li. Mendeleev. Commun. 31, 647(2021);
https://doi.org/10.1016/j.mencom.2021.09.018
[3] B. Wang, H. Song, X. Qu, J. Chang, S. Lu. Carbon dots as a new class of nanomedicines: op-

1342

portunities and challenges. Coordin. Chem. Rev. 442, 214010(2021);
https://doi.org/10.1016/j.ccr.2021.214010

[4] J. Mohsin, N. S. S. Ahmad, Ata-ur-R; A. Basit, F. Muhammad, A. A. Daniel, I. Zafar, M. A. Syed. Electrochim. Acta. 297, 250(2019); https://doi.org/10.1016/j.electacta.2018.11.167

[5] M. Nagaraj, S. Ramalingam, C. Murugan, S. Aldawood, Jun-O Jin, I. Choi, M. Kim. En-vironmental Research. 212, 113273(2022); https://doi.org/10.1016/j.envres.2022.113273

[6] P. Huang, S. J. Xu, M. Zhang, W. Zhong, Z. H. Xiao, Y. P. Luo. Mater. Chem. Phys. 240, 122158(2019); https://doi.org/10.1016/j.matchemphys.2019.122158

[7] W. Liu, H. P. Diao, H. H. Chang, H. J. Wang, T. T. Li, W. L. Wei. Sensor. Actuat. B-Chem. 241, 190(2017); https://doi.org/10.1016/j.snb.2016.10.068

[8] S. J. Zhao, M. H. Lan, X. Y. Zhu, H. T. Xue, T. W. Ng, X. M. Meng, C. S. Lee, P. F. Wang, W. J. Zhang. ACS. Appl. Mater. Interfaces. 7, 17054(2015); https://doi.org/10.1021/acsami.5b03228

[9] R. Atchudan, T. N. Jebakumar, I. Edison, M. Shanmugam, R. L. Yong. Physica. E. 126, 114417(2021); https://doi.org/10.1016/j.physe.2020.114417

[10] R. B. Wang, L. Jiao, X. L. Zhou, Z. Y. Guo, H. Y. Bian, H.Q. Dai. J. Hazard. Mater. 412, 125096(2021); https://doi.org/10.1016/j.jhazmat.2021.125096

[11] X. Y. Deng, Y. L. Feng, H. R. Li, Z. W. Du, Q. Teng, H. J. Wang. Particuology. 41, 94(2018); https://doi.org/10.1016/j.partic.2017.12.009

[12] X. Zhang, L. Z. Fu, Y. J. Hou, N. Long, G.Q. Zhu, X. F. Liao, L. D. Zhou, J. H. Lu, W. K. Kong. Ind. Crops. Prod. 177, 114439(2022); https://doi.org/10.1016/j.indcrop.2021.114439

[13] A. Paul, M. Kurian. Clea. Eng. Technol, 3, 100103(2021); https://doi.org/10.1016/j.clet.2021.100103

[14] B. Shi, Y. Su, L. Zhang, M. Huang, R. Liu, S.Zhao. ACS. Appl. Mater. Interfaces, 8, 10717(2016); https://doi.org/10.1021/acsami.6b01325

[15] F. Y. Du, J. N. Li, Y. Hua, M. M. Zhang, Z. Zhou, J. Yuan, J. Wang, W. X. Peng, L. Zhang, S. Xia, D. Q. Wang, S. M. Yang, W. R. Xu, A. H. Gong, Q. X. Shao. J. Biomed. Nanotechnol. 11, 780(2015); https://doi.org/10.1166/jbn.2015.2008

[16] M. Pan, Q. Y. Zheng, T. Wang, L. J. Liang, J. X. Mao, C. Zuo, R. C. Ding, H. S. Ai, Y. Xie, D. Si, Y. Y. Yu, L. Liu, M. L. Zhao. Nature. 600, 334(2021); https://doi.org/10.1101/2021.04.12.439291

[17] J. Z. Hou, W. X. Zhang, L. L. Li, X. P. Sun. Acta. Polym. Sin. 13, 30(2013); https://doi.org/10.3724/SP.J.1105.2013.12116

[18] M. J. Krysmann, A. Kelarakis, P. Dallas, E. P. Giannelis. J. Am. Chem. Soc. 134, 747(2012); https://doi.org/10.1021/ja204661r

[19] F. S. Niu, Y. L. Ying, X. Hua, Y. S. Niu, Y. H. Xu, Y. T. Long. Carbon. 127, 340(2018); https://doi.org/10.1016/j.carbon.2017.10.097

[20] B. S. B. Kasibabu, S. L. D'souza, S. Jha, S. K. Kailasa. Imaging of Bacterial and Fungal Cells Using Fluorescent Carbon Dots Prepared from Carica papaya Juice. J. Fluoresc. 25, 803(2015); https://doi.org/10.1007/s10895-015-1595-0

[21] S.Y. Zhao, X.P. Song, X.Y. Chai, P. T. Zhao, H. He, Z.W. Liu. J. Clean. Prod. 263,121561(2020); https://doi.org/10.1016/j.jclepro.2020.121561

[22] J. M. Zhang, X. X. Chen, Y. Li, S. Q. Han, Y. Du, H. Z. Liu. Anal. Methods-UK. 10, 541(2018); https://doi.org/10.1039/C7AY02806G

[23] A. Ra, A. Tnjie, B. Sp, S. S. Clament. J. Photoch. Photobio. A. 372, 99(2019); https://doi.org/10.1016/j.jphotochem.2018.12.011

[24] L. Zhao, Y. S. Wang, X. H. Zhao, Y. J. Deng, Y. Z. Xia. Polymers. 11, 1731(2019); https://doi.org/10.3390/polym11111731

[25] M. F. B. Mirza, Y. C. Chen. J. Colloid. Interf. Sci. 501, 341(2017); https://doi.org/10.1016/j.jcis.2017.04.045

[26] J. Zhong, X. M. Chen, M. R. Zhang, C. X. Xiao, L. L. Cai, W. A. Khan, K. X. Yu, J. Y. Cui, L. He. Chinese. Chem. Lett. 31, 201(2020); https://doi.org/10.1016/j.cclet.2020.01.007

[27] H. Eskalen, S. Uru, A. Hakan, ükrü. zgan, S. Bahattin. Ind. Crop. Prod. 147, 112209(2020); https://doi.org/10.1016/j.indcrop.2020.112209

[28] Y. Ran, S. Y. Wang, Q. Y. Yin, A. L. Wen, S. Chen. Luminescence. 35, 870(2020);

https://doi.org/10.1002/bio.3794

[29] S. M. Song, J. H. Hu, M. L. Li, X. J. Gong, C. Dong, S. M. Shuang. Mat. Sci. Eng. C-Mater. 118, 111478(2021); https://doi.org/10.1016/j.msec.2020.111478

[30] M. D. Zheng, C. G. Wang, Y. Y. Wang, W. Wei, S. Ma, X. H. Sun, J. He. Talanta. 185, 309(2018); https://doi.org/10.1016/j.talanta.2018.03.066

[31] R. Dineshkumar, S. Devikala. Mater. Today. Proc. 34, 488(2021); https://doi.org/10.1016/j.matpr.2020.03.096

[32] M. Lu, Y. Duan, Y. Song, J. Tan, Z. Li. J. Mol. Liq. 269, 766(2018); https://doi.org/10.1016/j.molliq.2018.08.101

[33] N. K. Sahoo, G. C. Jana, M. N. Aktara, S. Das, M. Hossain. Mat. Sci. Eng. C-Mater. 108, 110429(2019); https://doi.org/10.1016/j.msec.2019.110429

[34] P. Bilgehan, B. Ebru. Res. Chem. Intermediat. 47, 1865(2021); https://doi.org/10.1007/s11164-021-04404-y

[35] Y. Zhang, Z. Y. Gao, X. Yang, J. L. Chang, Z. Y. Liu, K. Jiang. RSC. Adv. 9, 940(2019); https://doi.org/10.1039/C8RA09471C

[36] R. Liu, Y. Zhang, P. G. Piao, L. Y. Meng. Carbon. Lett. 31, 821(2021); https://doi.org/10.1007/s42823-020-00222-1

[37] J. Shen, S. M. Shang, X. Y. Chen, D. Wang, Y. Cai. Mat. Sci. Eng. C-Mater. 76, 856(2017); https://doi.org/10.1016/j.msec.2017.03.178

[38] A. Ams, B. Eb. Microchem. J. 159, 105357(2020); https://doi.org/10.1016/j.microc.2020.105357

[39] L. Zhao, Y. S. Wang, X. H. Zhao, Y. J. Deng, Y. Z. Xia. Polymers. 11, 1731(2019); https://doi.org/10.3390/polym11111731

[40] X. Zhang, C. Li, S. Zhao, H. Pang, Z. Li. Opt. Mater. 110, 110461(2020); https://doi.org/10.1016/j.optmat.2020.110461

[41] A. Natarajan, R. Murugesan, S. Chellappan, S. Thangasamy, K. Ponnuchamy, S. L. Yun, K. S. Ramakrishnan. Environ. Res. 119, 111263(2021); https://doi.org/10.1016/j.envres.2021.111263

[42] F. Ricchelli. Journal of photochemistry and photobiology. B, Biology. 3, 289(1989); https://doi.org/10.1007/BF01134381

[43] L.Y. Fang. China University of Petroleum. (2019);